Supporting Information

for

Title: Flexible crystalline β-Ga_2O_3 solar-blind photodetectors

*Junyu Lai, Md Nazmul Hassan, Edward Swinnich, Zhao Tang, Sang-Ho Shin, Munho Kim, Peihong Zhang, Jung-Hun Seo**

Creation of β-Ga_2O_3 Nanomembrane

The creation of the β-Ga_2O_3 NMs began with a Sn-doped β-Ga_2O_3 bulk that was grown by molecular beam epitaxy and highly doped with Sn around $1x10^{18}$ cm^{-3}.Then β-Ga_2O_3 NMs were then produced by clipping several large segments from the bulk substrate at an angle of 77°, followed by an exfoliation using a well-known taping method. β-Ga_2O_3 segments were easily mechanically exfoliated in [100] direction due to the weak binding energy in this direction. After several times of exfoliation, we transfer β-Ga_2O_3 flakes to SiO_2 substrate to create sub-micron thick β-Ga_2O_3 (β-Ga_2O_3 NMs) by the sonification process in isopropyl alcohol.

N and k value measurement

After permanently bond the β-Ga_2O_3 NMs onto the plastic substrate, we use Filmetric F40 -film thickness & n,k measurement system to measure the n,k value of β-Ga_2O_3 NMs under bending condition. In order to apply uniaxial compressive and tensile strain onto β-Ga_2O_3 NMs. We design convex and concave molds that have different curve radii from 110 to 20 mm which corresponds to up to 0.33% of the tensile strain (for the convex mold) and up to 0.19% of the compressive uniaxial strain (for the concave mold). The bending test was first performed on the concave mold to apply uniaxial compressive strains from the flat condition to 0.06%, 0.09%, and 0.19%, followed by uniaxial tensile strains from the flat condition to 0.09%, 0.13%, 0.19%, and 0.33%, respectively.

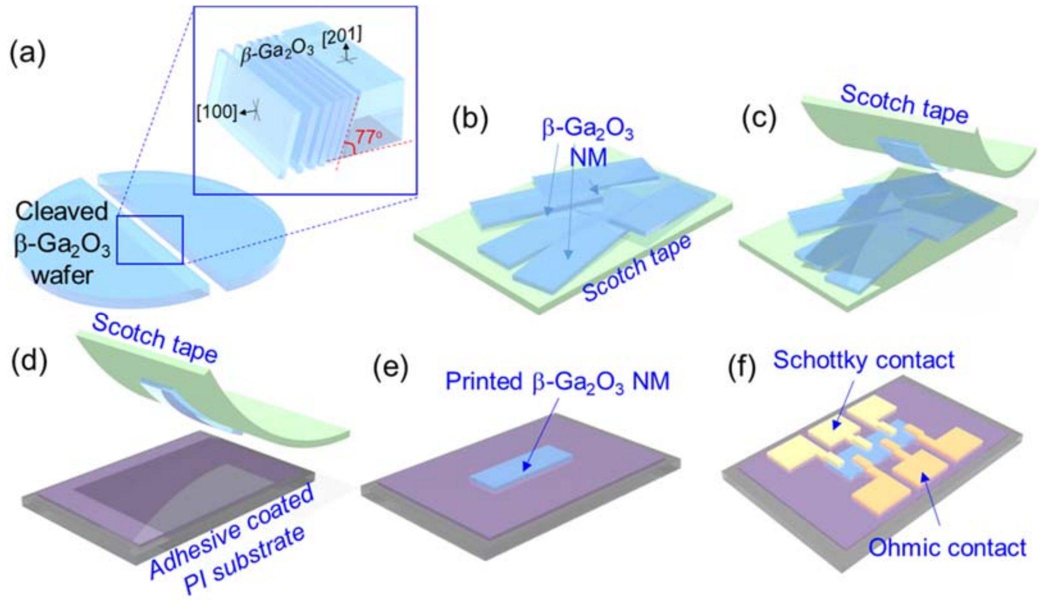

Figure S1. A schematic illustration of the fabrication process for the β-Ga_2O_3 NM PDs; **(a)** a cleaving process from bulk β-Ga_2O_3, **(b),(c)** an exfoliation process to further thin down β-Ga_2O_3 NM, **(d),(e)** a micro-transfer printing process to relocate the β-Ga_2O_3 NM onto a plastic substrate, **(f)** metallization process for ohmic and Schottky contacts.

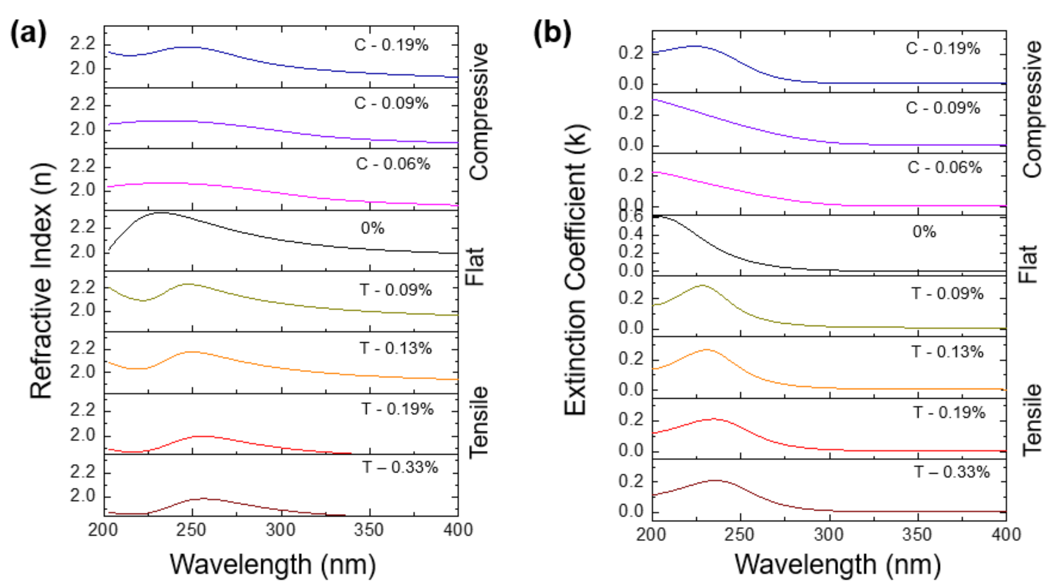

Figure S2. **(a)** The refractive index as a function of wavelength on PI substrate under tensile and compressive strain. **(b)** The extinction coefficient as a function of wavelength on PI substrate under tensile and compressive strain.

Table S1. Optical band gap of β-Ga_2O_3 NMs under compressive and tensile strain extracted from the refractive index and the extinction coefficient in Figure S1.

Compressive Strain		
Bending Radius	Strain%	Band gap(eV)
flat	0	4.92
110mm	0.06	4.85
75mm	0.09	4.82
35mm	0.187	4.75

Tensile Strain		
Bending Radius	Strain%	Band gap(eV)
flat	0	4.92
75Tmm	0.09	4.85
50Tmm	0.127	4.83
35Tmm	0.187	4.73
20Tmm	0.32	4.7

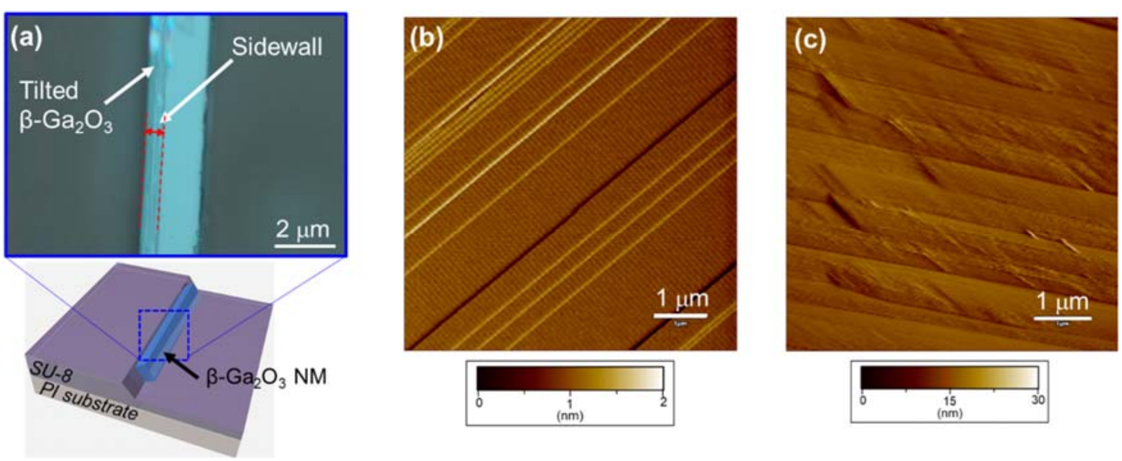

Figure S3. (a) A microscopic image of the tiled transfer-printed β-Ga_2O_3 NMs on a plastic substrate. An illustration below is to aid to show the tilted β-Ga_2O_3 NMs on a substrate. Angled AFM images of β-Ga_2O_3 NMs on PI substrate **(b)** before and **(c)** after bending (50 times). The scale bar is 1um.

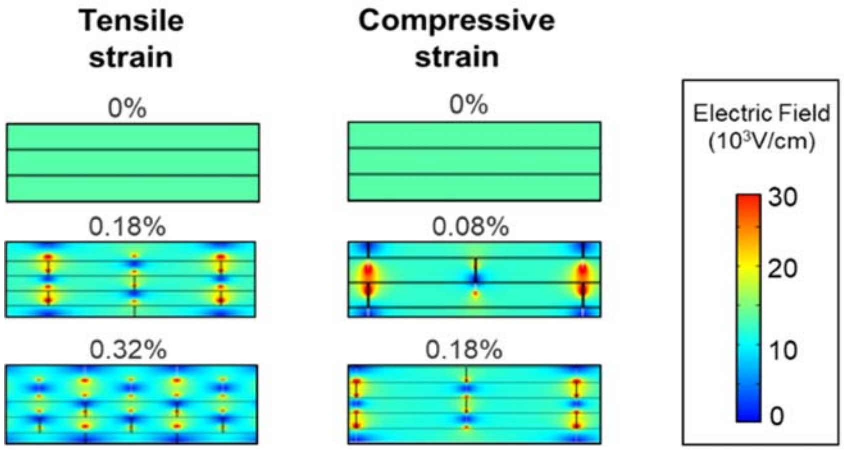

Figure S4. A simulated electric field distribution in β-Ga_2O_3 NM under different strain conditions showing an existence of different degrees of strain-

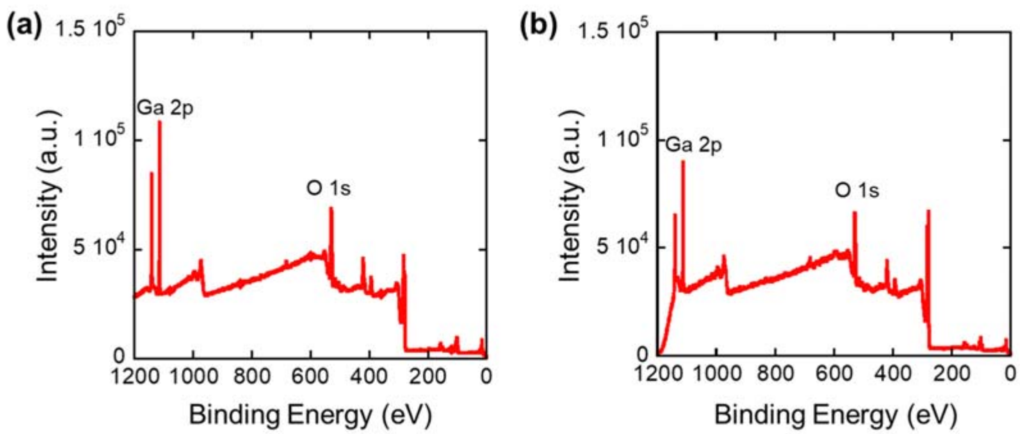

Figure S5. XPS characterization of **(a)** as-fabricated β-Ga_2O_3 NM and **(b)** fractured β-Ga_2O_3 NM.